Письма в ЭЧАЯ. 2005. Т. 2, № 6(129). С. 87–97

УДК [51-72:530.145]+[51-72:541.1]

MOLECULAR DYNAMICS SIMULATIONS ON STRUCTURAL CONFORMATIONS OF RHODOPSIN AND PRION PROTEINS

Kh. T. Kholmurodov[1]

Joint Institute for Nuclear Research, Dubna

Molecular dynamics simulations were performed to investigate the structural conformation of the rhodopsin and prion proteins. We have estimated the effect of specific disease-related amino acid mutations on the dynamics and conformational changes.

Молекулярно-динамическое моделирование выполнено с целью исследования структурных конформаций белков родопсина и преонов. Исследованы эффекты замещения аминокислот, связанные с возникновением заболеваний, на динамику и конформационные изменения белков.

INTRODUCTION

In the present study we have employed the molecular dynamics (MD) simulation to investigate conformation dynamics of the rhodopsin and prion proteins. We have estimated the effect of the specific disease-related amino acid mutations on the structural conformation of the above proteins.

Retinal proteins (rhodopsins), a superfamily of the membrane receptors (known as GPCRs, G-protein-coupled receptors), are involved in conversion of light to chemical energy and vision. The outer layer of the retina segment comprises about 130 million photoreceptor cells (rods and cones), providing chromatic (color) images of high spatial resolution and achromatic vision with less spatial resolution. All rhodopsins contain the molecule retinal as their chromophore, and the activation of rhodopsins is initiated during a very short time (200 fs) through photoinduced isomerization events of the retinal chain around specific double bond. The rhodopsin (Rh) is composed of seven-transmembrane helical protein, opsin, and of retinal, a polyene chain bound to the protein through protonated Schiff base linkage to Lys^{296}. The mature form of the biomolecule Rh is comprised of 338 amino acid residues in total, and its high-resolution crystal structure is available. Resonance Raman-spectroscopy experiments on Rh photoisomerization discovered that the light energy during the absorption of photon energy and Rh photocycle is stored through a chromophore structural distortion. Time-resolved UV/VIS spectroscopy measurements have shown that Rh photocycle process involves several intermediates [1–4]. Consequently, many recent computer molecular studies have been aimed at the theoretical description of the Rh isomerization and its conformational relaxation

[1]The temporary research position where investigations are performed: Computational Astrophysics Laboratory, Advanced Computing Center, RIKEN (The Institute of Physical and Chemical Research), Hirosawa 2-1, Wako, Saitama 351-0198, Japan.

processes [5–9]. In [9], for example, MD simulations have been performed on Rh model embedded in the lipid bilayer and water environment. Retinal was isomerized around $C_{11} = C_{12}$ double bond, changing its conformation from 11-*cis* to all-*trans*, in accordance with the experimental observations. However, the nature of nonreaction dynamics and conformation of the Rh is still unknown. It is also worth noting that dynamics of retinal photoisomerization is strongly influenced by its environment (opsin + solvent). The correlation of the Rh conformational dynamics and its activation process at later stages are the most challenging targets in computer molecular modeling of Rh. The relative movement of the Rh helices could be part of the Rh light-activated photocycle. The expriments revealed that movement of Rh helices (for example, a movement of helix VI relative to other helices) plays a key role in Rh activation. This evidently motivates the extremely time-consuming atomic modelling of Rh. There has been considered that the large-scale motion of Rh may be a common dynamic motion for other alpha-helical G-protein receptors [10–12, 5]. In the present work we investigated the Rh conformation dynamics in the dark-adapted state. The 3-ns MD simulations have been performed on Rh to study its conformation behavior in an explicit (water) solvent [13]. We were also aimed to estimate the induced effect of the specific, disease-related amino acid point mutations (for example, E134N and others [2, 3, 5]) on the Rh conformation.

The structural and functional properties are known often to correlate well for a number of proteins. This fact can be obviously observed, for example, for the prion proteins. It is well understood that the misshapen prion protein (today cell biology's challenging topic) is generally associates with its disease-related form. In the normal human prion protein (PrP) the prion molecules are coiled into helix and help to maintain the integrity of the nerve cells. As theoretical and experimental observations show, the infectious prion proteins are more sheet-like and coax normal prions to fold into infectious (disease-related) form [14,15]. Thus, a central question of the physiological functionality of the normal prion protein (PrP^C) and its aberrant form (PrP^{Sc}) has to be closely connected with their structural transformations. In [16–18] we have performed MD simulations on the human PrP to elucidate the effect of point mutations related to the inherited Creutzfeldt–Jakob disease (CJD). We examined and compared the structural changes of the human PrP through the consideration of three NMR structures (the wild-type prion and two mutant structures with $Glu^{200} \rightarrow$ Asp and $Glu^{200} \rightarrow$ Lys substitutions). In this study we present the structural analysis and residue distance distributions in detail.

1. THE PRIMARY PHOTOINDUCED ISOMERIZATION OF RHODOPSIN

The analysis of the electron density data on the 11-*cis*-retinal chromophore and transmembrane helices [1, 2] provides some preliminary picture of the intermolecular interactions in the Rh protein. In Fig. 1 the Rh ribbon structure with a retinal chromophore is presented. From the intradiscal side of the Rh the retinal chromophore has been positioned in a way that it equally separates the protein into the cytoplasmic and extracelullar regions. The structural conformation of the retinal chromophore in Rh has to be stabilized by a number of the interhelical hydrogen bonds and hydrophobic interactions (dominantly by helices I–V of the Rh). Most of the interhelical interactions (in helices I–V) are mediated by highly conserved residues in G-protein-coupled receptors (GPCRs). A binding pocket environment of the

11-*cis*-retinal chromophore from the Rh cytoplasmic part are the important intermolecular side chains, surrounding the 11-*cis*-retinylidene group [1–3].

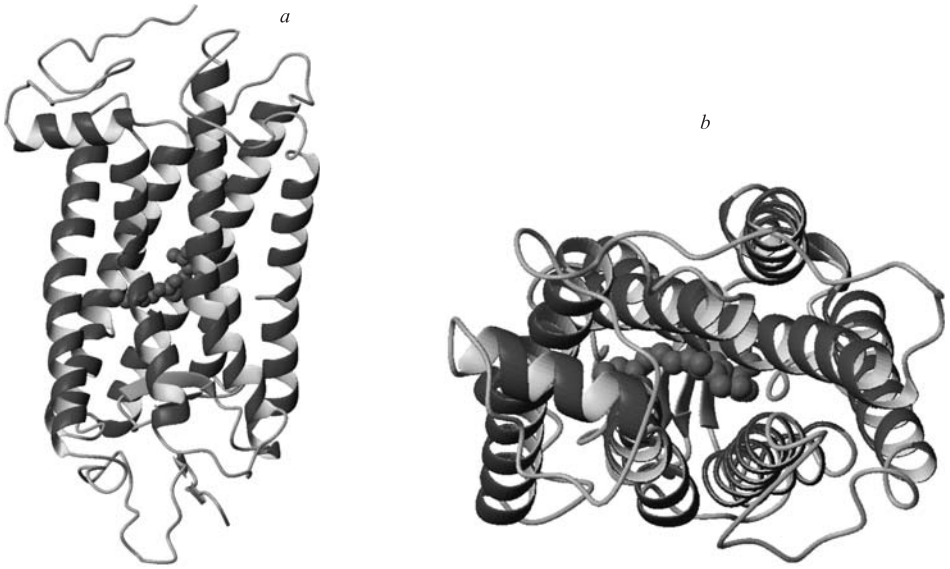

Fig. 1. The Rh ribbon structure and chromophore at the initial state: *a*) view from the extracellular side; *b*) view from the cytoplasmic side. The retinal polyene chain is drawn as balls

The structural conformations of the Rh essentially determine its function as a light-activated receptor. In the dark state we have a Rh + 11-*cis* retinal configuration. Photoinduced isomerization of the chromophore results in Rh + all-*trans* retinal state. In the dark state the (11-*cis*) retinal stabilizes the inactive conformation of Rh. Its isomerization (all-*trans*) triggers Rh transition to an active state, which catalyzes the GDP/GTP exchange. Thus, the chromophore conformational change from the 11-*cis* to all-*trans* triggers a transition of the Rh receptor to the active state, initiating the exchange of the GDP for GTP in α subunit of the transducin, a G protein associated with Rh [2, 9].

It is worth noting that the rhodopsin (Rh), bacteriorhodopsin (bR) and halobacteria rhodopsin (hR) are members of the transmembrane proteins family, which show similar conformational properties. They possess, viz.:

- the same number of transmembrane helices;
- the topography of the polypeptide chain arrangement across the lipid bilayer;
- the position of the lysine side chain to which retinal is attached.

The structure and functions of Rh and bR (hR), however, are completely different from each other. For example, the bR conformation (a light-driven proton pump) in the light-adapted state is a bR + all-*trans* retinal. Through the bR photoisomerization process we have a bR + 13-*cis* retinal state, which is a structurally different configuration in comparison with the Rh as described above. Also, the bR transition from all-*trans* to 13-*cis* configuration

triggers a photocycle process in which one proton is pumped from the cytoplasmic side to the extracellular part of the membrane.

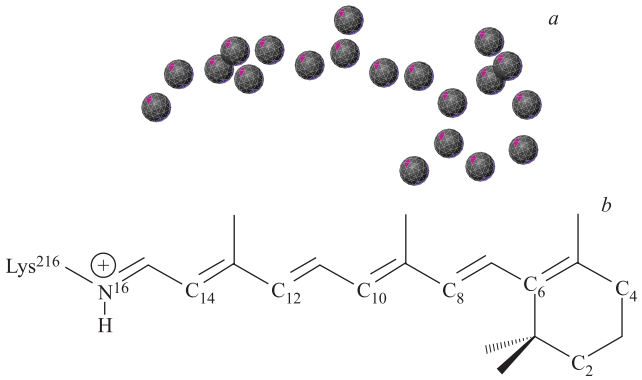

Fig. 2. A molecular structure (*a*) and a schematic diagram (*b*) of a retinal chromophore. The positions of the beta-ionone (right) ring and Schiff-base linkage (left) are shown

In Fig. 2, *a* a molecular structure diagram of a retinal chromophore is presented. Figure 2, *b* displays a retinal polyene chain with six double bonds, bounded to Lys^{216} (Lys^{296} for Rh) via a Schiff base. As the resonance Raman-spectroscopy experiments have shown, the light energy in Rh is stored through structural distortion of the retinal chromophore [1, 3]. The activation of the Rh is initiated, as was noted above, by a retinal photoisomerization around a specific double bond ($C_{11} = C_{12}$ in Rh, $C_{12} = C_{13}$ in bR, etc.). The Rh photocycle process involves several intermediates [3], which are detected experimentally at the cryogenic and room temperatures (PHOTO-Rh (570 nm absorption spectra, within 150 ns), BATHO-to-BSI (529 nm absorption spectra and 5 ps), LUMI (μs), META-I (ms) and META-II). The retinal binding pocket has to be large and flexible enough to accomodate a variety of chromophores [2, 9]. Its large motion is accompanied, for example, with BATHO-to-BSI transition or implies the rotation of helix IV [4]. Thus, the retinal binding sites or salt bridges in the Rh are evidently correlated with the activation mechanism of the protein. For example, the Rh activation is associated with a shift of the relative orientation of helices III and VI [5, 9]. The Schiff group and Glu^{113} binding stabilize the connection between helices III and VII, the disruption of this binding site activates Rh in the absence of the retinal chromophore. In later photoisomerization stages (META-I and META-II intermediates) the major conformational changes of the Rh have to occur. Finally, in META-II the Schiff-base proton has to transfer to the Glu^{113} amino acid [3, 19, 20].

2. MD SIMULATIONS ON THE RHODOPSIN STRUCTURAL CONFORMATIONS

We simulated the bovine Rh to study its conformation dynamics in the dark-adapted state. The molecular mechanics (MM) and MD simulations on Rh were performed with an explicit (water) solvent. A molecular model was constructed from the Rh crystal structure (PDB: 1HZX) (the simulation methods to be described in detail elsewhere). Briefly, two sets of

MD simulations (viz., cutoff and no cutoff calculations) were performed with the software package AMBER (cutoff method: version 5.0, Parm94 on a supercomputer Fujitsu VPP; no cutoff method: modified version 7.0, Parm96 on a special-purpose computer MDGRAPE-2 [21, 22]). The temperature was kept constant by using Berendsen algorithm with a coupling time of 0.2 ps; the cutoff distance of nonbonded interactions was 14 Å; for the MDGRAPE-2 all interactions were calculated. The integration time step in the MD simulations was 1 fs. The simulation procedures were the same in all calculations. Firstly, a potential energy minimization was performed on an initial state for each system. Next, the MD simulation was performed on the energy-minimized states. The temperatures of the considered systems were gradually increased by heating to 300 K and then kept at 300 K for the next 3 million time steps. The trajectories at 300 K for 3.0 ns were compared and studied in detail.

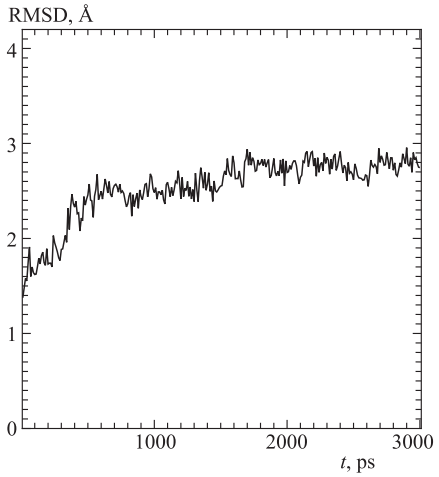

Fig. 3. The RMSD (root-mean-square displacement) for the Rh total structure domain within 3-ns state

Figure 3 shows the root-mean-square deviation (RMSD) for a total structure domain of the Rh protein. In Fig. 4 the RMSD values separately calculated for each of helices I–VII are presented. The RMSD values were evaluated for only the backbone atoms of the helices. The RMSD of the total Rh structure, as seen from Fig. 3, has been kept around 4.5 Å, which indicates a stability of the Rh structure during the 3.0-ns period of simulations. With regard to a selected Rh helix (Fig. 4) we observe a relative movement of Rh helices; displacements of Rh helices do not behave similarly. Helices I, III and V exhibit the highest deviations from the reference structure.

In Fig. 5, *a* the superposition of the representative structures is presented at 3-ns state. Figure 5, *b* shows the largest displacements from the reference structure for helices III and V. The largest differences are seen in the cytoplasmic region of the helices; the extracellular ends show slight movement. Some reported MD studies indicate, for example, the largest RMSDs for helices I, V and VI or helices IV, V and VI [5, 10, 11]. It is worth noting that spin-label experiments show the movement of the cytoplasmic part for helices II, VI and VII [9, 12].

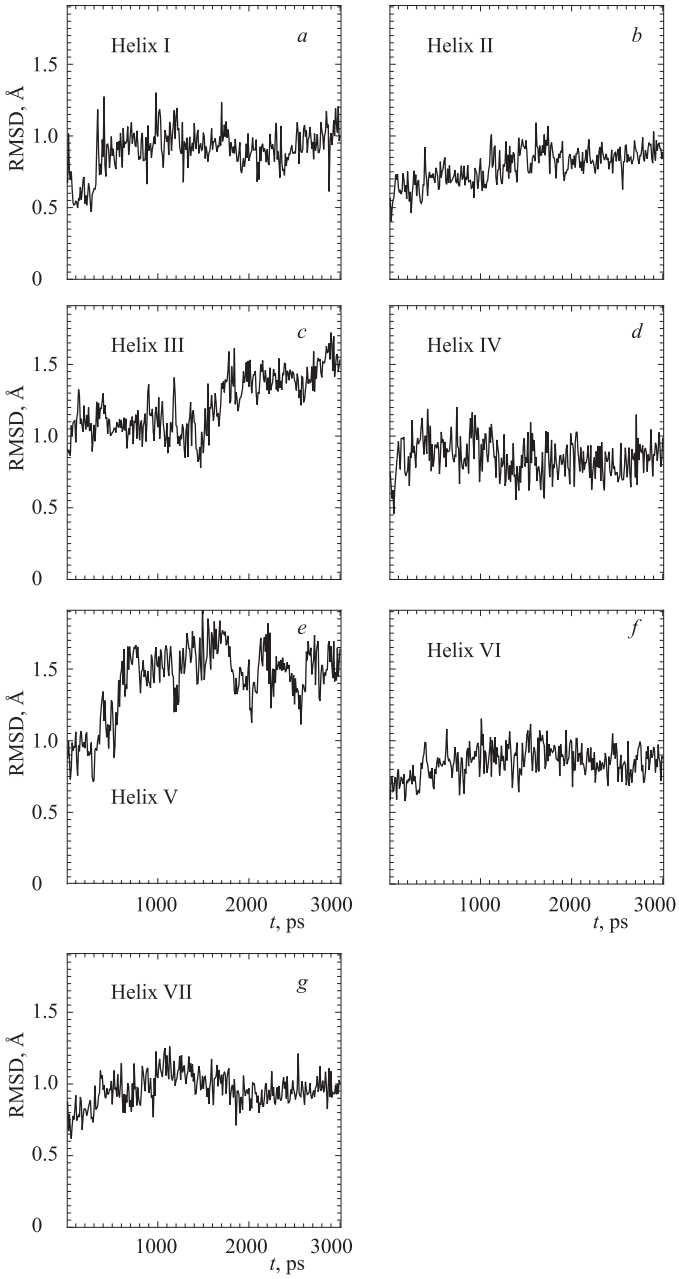

Fig. 4. The RMSDs for helices I–VII of Rh. The relative movement of the helices results in nonlinear behavior between the RMSDs. The largest deviations are seen for helices I, III and V

Next we have simulated the effect of the E134N mutation on the Rh conformation dynamics. The Glu134N mutation has been regarded as an important site from the point

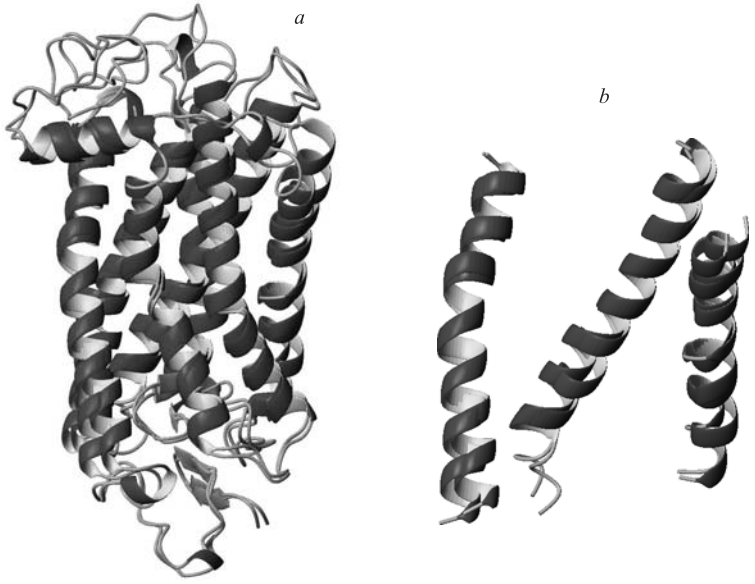

Fig. 5. *a*) The Rh ribbon structure at the initial and final (3-ns) states. *b*) The largest distortions are observed for helices I (left), III (middle) and V (right)

of view of Rh protonation mechanism. For example, this mutation can activate transducin in the absence of the 11-*cis* retinal [3]. In Fig. 6 the RMSD evolutions for the normal Rh and with E134N mutation are shown. In Fig. 7 the RMSD values for each of helices I–VII for both normal and mutant E134N Rh are presented. The comparison of the above pictures indicates that generally the reference and E134N mutant structures behave similarly. It is worth noting that nearly every residue in Rh has been examined with site-directed mutagenesis [11, 12]. There have been several important amino acids (E134N, E122Q, D83N, etc.) to play an essential role in the Rh protonation mechanism mentioned above. Although some molecular simulation results have been reported (see, for example, [5]), which suggest that the nature of dynamical transitions in Rh dark-adapted state has been governed by its collective motion and no single amino acid or particular defined sequence has been considered to be dominant. However, ample experimental evidence ([2, 3], etc.) reveals that a selected amino acid mutation may cause essential changes in the formation of Rh intermolecular interactions, mostly electrostatics. The presented simulation results support in general this statement.

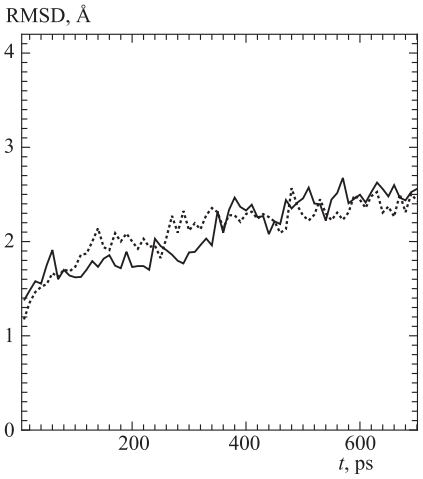

Fig. 6. The RMSD for the reference structure (solid line) and Rh with E134N exchange (dotted line) within 1-ns state

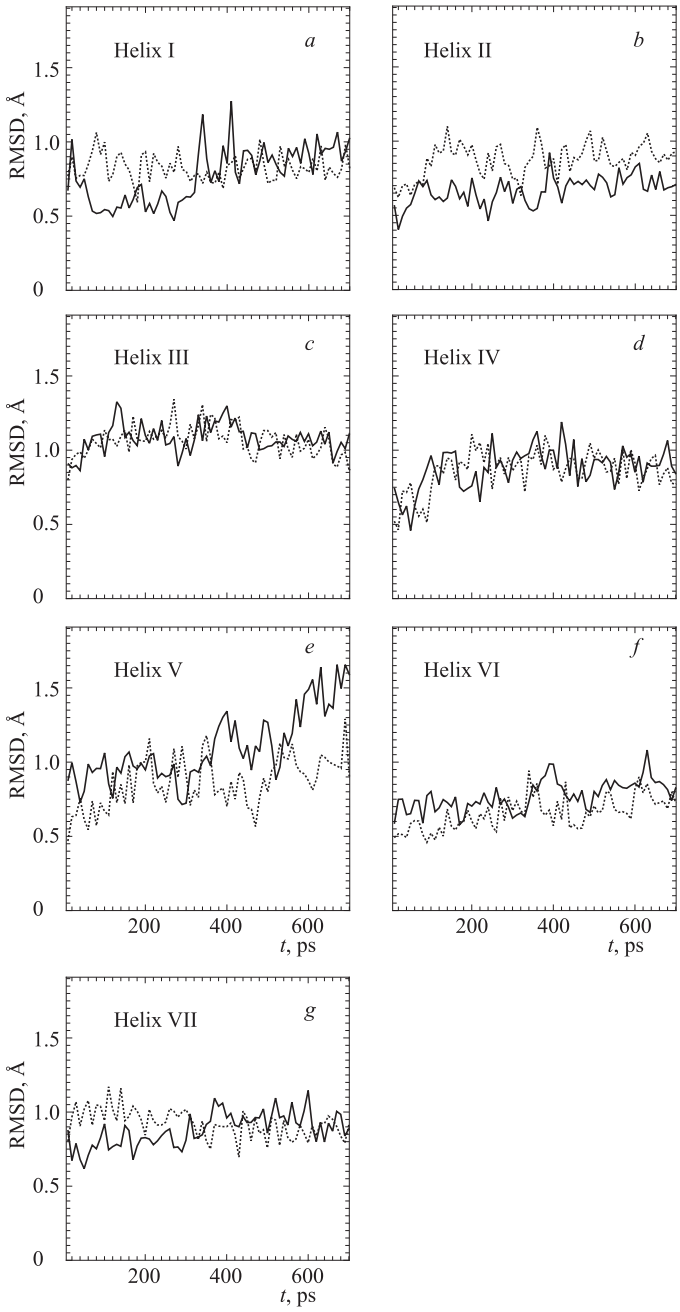

Fig. 7. The RMSDs for helices I–VII for the reference structure (solid line) and Rh with E134N exchange (dotted line) within 1-ns state

3. MD SIMULATIONS ON THE DYNAMICS AND CONFORMATIONAL CHANGES OF PRION PROTEINS

The mature form of the human PrP is comprised of 208 residues (numbered 23–230). The C-terminal part of the polypeptide chain with residues 125–228 forms a compact globular domain and is stable, whereas the N-terminal part (21–124) is unstructured in aqueous solution at pH5. The C-terminal region containing domain (125–228) is displayed in Fig. 8. We have performed MD simulations on three model structures of the human PrP. Model 1 is derived from the NMR structures of the human PrP (PDB code: 1QM2). The model includes a prion globular domain (a structured part, residues 125–228), and we called model 1 a «wild-type structure». Models 2 and 3 represent mutant structures containing $Glu^{200} \rightarrow Asp$ and $Glu^{200} \rightarrow Lys$ substitutions. These two models are built from the same NMR structure as for model 1. $Glu^{200} \rightarrow Lys$ in model 3 is a disease-related amino acid exchange, so we call this model an «abnormal-type structure». The wild-type PrP has a glutamate at 200 codon, the $Glu^{200} \rightarrow Asp$ and $Glu^{200} \rightarrow Lys$ substitutions occur just before the third helix (a longer, middle helix in Fig. 8). We have used the program package AMBER 5.0 to perform the MM potential energy minimizations and MD simulations. The nonbonded interactions were calculated using the cutoff method ($r_{\mathrm{cut}} = 14$ Å).

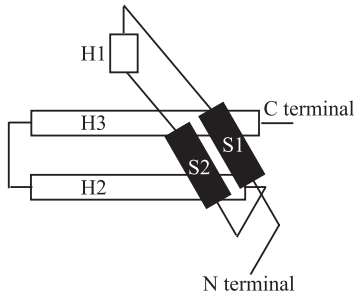

Fig. 8. A schematic diagram of globular domain of the human PrP. The structure consists of three α helices (H1, H2, and H3) and a short β sheet (S1 and S2)

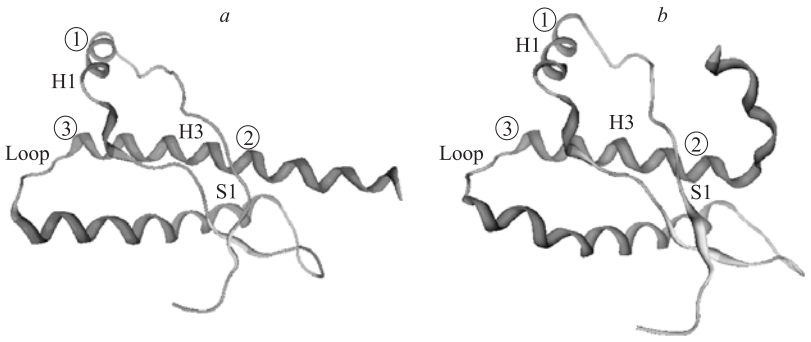

Fig. 9. The structure plots of the human PrP in model 3 (mutant $Glu^{200} \rightarrow Lys$ prion protein) for the initial (*a*) and final (*b*) states (1.6 ns)

Figure 9 shows the calculated structures for model 3 (mutant $Glu^{200} \rightarrow Lys$ prion protein) at the initial (*a*) and final (*b*) states. As is seen from Fig. 9, the structure of the mutant $Glu^{200} \rightarrow Lys$ prion has partly rearranged; we observe a collapse of the third (longest) α helix H3. A structure destruction position is on residue 219, where H3 rearranges to interact with the strand between H1 and S1. For the wild-type prion, as analysis shows (the data are not shown), the globular domain is maintained stable during the whole simulation period. A comparison of the pictures for the wild and abnormal $Glu^{200} \rightarrow Lys$ type prions

suggests a mechanism of the structural reorganization as decribed above. Namely, when a glutamate-to-lysine substitution occurs (at the mutation point 200) H1 and H3 come very close to each other. A flexible motion of H1 to H3 seems to result in the protein structural rearrangement. At the same time H3 interacts with the strand between H1 and S1 and forms probably a new hydrogen bond. As regards model 2 (mutant $Glu^{200} \rightarrow$ Asp prion), its initial structural changes look almost the same as for model 3. The longest α helix H3 begins to bend at residue 219, in the same way as in model 3. However, the structure will not collapse completely, its final behavior is not like that in Fig. 4, so the protein refolds properly.

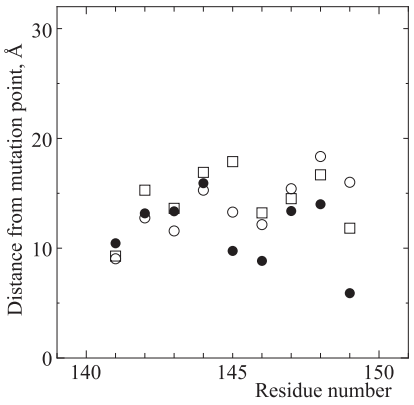

Fig. 10. The residue distance distributions for the final state (1.6 ns). The distances are shown between the atoms at the α helix H1 (residues 141–149) at the mutation point 200: ○ — model 1 (normal-(wild-)type prion protein); □ — model 2 (mutant $Glu^{200} \rightarrow$ Asp protein); ● — model 3 (mutant $Glu^{200} \rightarrow$ Lys protein)

The analysis of the prion structures indicates that flexibility of the short α helix H1 is very sensitive to the type of amino-acid substitution at the residue point 200. For the $Glu^{200} \rightarrow$ Lys mutation all the atomic positions of H1 look very close to the α helix H3 (in contrast with the other two protein models under consideration). We estimated the residue distance distributions of the α helix H1 in detail. The H1 consists of 9 residues (numbered 141–149), for all of them we have calculated the atomic distance distributions to the mutation point 200. In Fig. 10 the calculated distances between all the atoms of the residues at H1 and that of residue 200 for the final (1.6 ns) state are displayed. Figure 10 shows the minimum distance distributions between the atoms of H1 and residue 200. It is clear that all the three models at the beginning of MD simulations have a similar atomic distance distribution. However, the farther simulation proceeds the more greatly distance distributions differ one from another. The residue distance distributions of models 1 and 2 look similar. As for model 3, in the final structure the atoms of the α helix H1 are positioned very close to the mutation point 200. Thus, a strong contact between the α helices H1 and H3 causes H3 to be misfolded in particular and the protein structure as a whole [23].

REFERENCES

1. *Okada T. et al.* // J. Struct. Biol. 2000. V. 130. P. 73–78.
2. *Palczewski K. et al.* // Science. 2000. V. 289. P. 739–745.
3. *Kandori K., Shichida I., Yoshizawa T.* // Biokhimiya. 2001. V. 66. P. 1483–1498.
4. *Pan D., Mathies R. A.* // Biochem. 2001. V. 40. P. 7929–7936.
5. *Crozier P. S. et al.* // J. Mol. Biol. 2003. V. 333. P. 493–514.
6. *Humphrey W. et al.* // Biophys. J. 1998. V. 75. P. 1689–1699.

7. *Tajkhorshid E. et al.* // Biophys. J. 2000. V. 78. P. 683–693.

8. *Hayashi S., Tajkhorshid E., Schulten K.* // Biophys. J. 2002. V. 83. P. 1281–1297.

9. *Saam J. et al.* // Ibid. P. 3097–3112.

10. *Farahbakhsh Z., Hideg K., Hubbell W.* // Science. 1993. V. 262. P. 1416–1419.

11. *Hubbell W., Cafiso D., Altenbach C.* // Nature Struct. Biol. 2000. V. 7. P. 735–739.

12. *Altenbach C. et al.* // Biochem. 2001. V. 40. P. 15493–15500.

13. *Kholmurodov K., Ebisuzaki T.* // ICMS-CSW2004, Tsukuba, 2004. V. C4. P. 9–11.

14. *Prusiner S. B.* // Trends Biochem. Sci. 1996. V. 21. P. 482–487.

15. *Aguzzi A., Weissmann C.* // Nature. 1997. V. 389. P. 795–812.

16. *Kholmurodov K., Okimoto N., Ebisuzaki T.* // 16th Meeting of Molecular Simulation Society of Japan (MSSJ), Niigata, Japan, Dec. 2003.

17. *Kholmurodov K., Okimoto N., Ebisuzaki T.* // RIKEN Rev. 2002. V. 48. P. 16–18.

18. *Kholmurodov K. et al.* // Meetings Abstr. Jap. Phys. Soc. (JPS). 2002. V. 57. P. 293.

19. *Kuwata O. et al.* // Biokhimiya. 2001. V. 66. P. 1588–1608.

20. *Sheikh S. P. et al.* // Nature. 1996. V. 383. P. 347–350.

21. *Narumi T. et al.* // Mol. Simul. 1999. V. 21. P. 401–408.

22. *Okimoto N. et al.* // Chem-Bio Inform. J. 2003. V. 3, No. 1. P. 1–11.

23. *Kholmurodov K. T. et al.* // Ibid. V. 3, No. 2. P. 86–95.

Received on May 19, 2004.